

## SUPPORTING INFORMATION

# MM Quadruply Bonded Complexes Supported by Vinylbenzoate Ligands: Synthesis, Characterization, Photophysical Properties and Application as Synthons

5    **Samantha E. Brown-Xu, Malcolm H. Chisholm,\* Christopher B. Durr,  
Thomas F. Spilker and Philip J. Young**

### Table of Contents

10 S1 – S2.....	NIR Emission
S3 – S13.....	fs-Transient Absorption and kinetics
S14 – S24.....	ns-Transient Absorption and kinetics
S25.....	fs-Time Resolved Infrared of <b>2B</b>
S26.....	Kinetic trace of <b>4A</b>
15 S27 – S32.....	<sup>1</sup> H NMR in d <sub>8</sub> -THF at room temperature
S33 – S38.....	High resolution MALDI-TOF Mass Spec
S39.....	Comparison of experimental and theoretical electronic transitions
S40.....	Crystallographic Data Collection Parameters for <b>1A</b> and <b>2A</b>

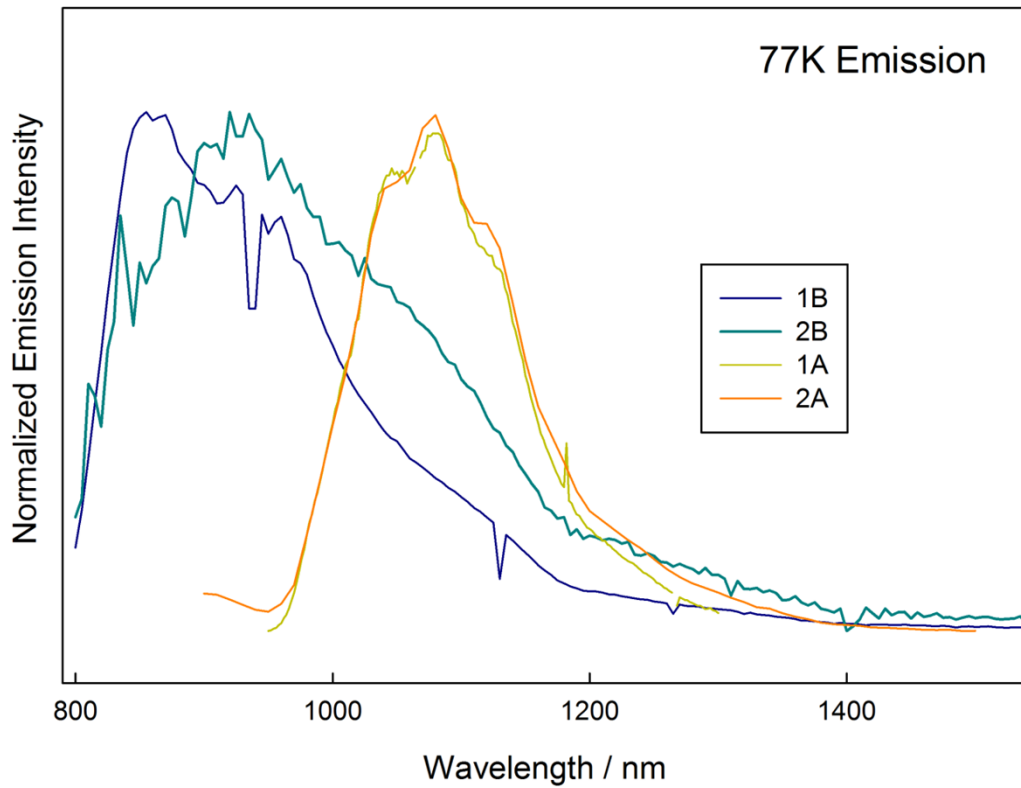


Figure S1. NIR emission of **1A**, **1B**, **2A**, and **2B** in 2-MeTHF at 77K.

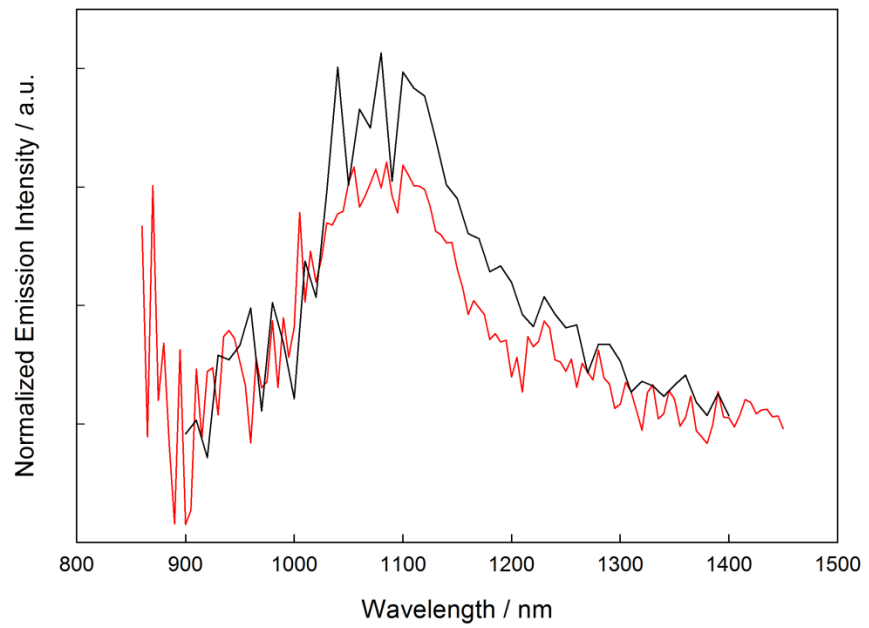


Figure S2. NIR emission of **3A** (black) and **4A** (red) in 2Me-THF at room temperature.

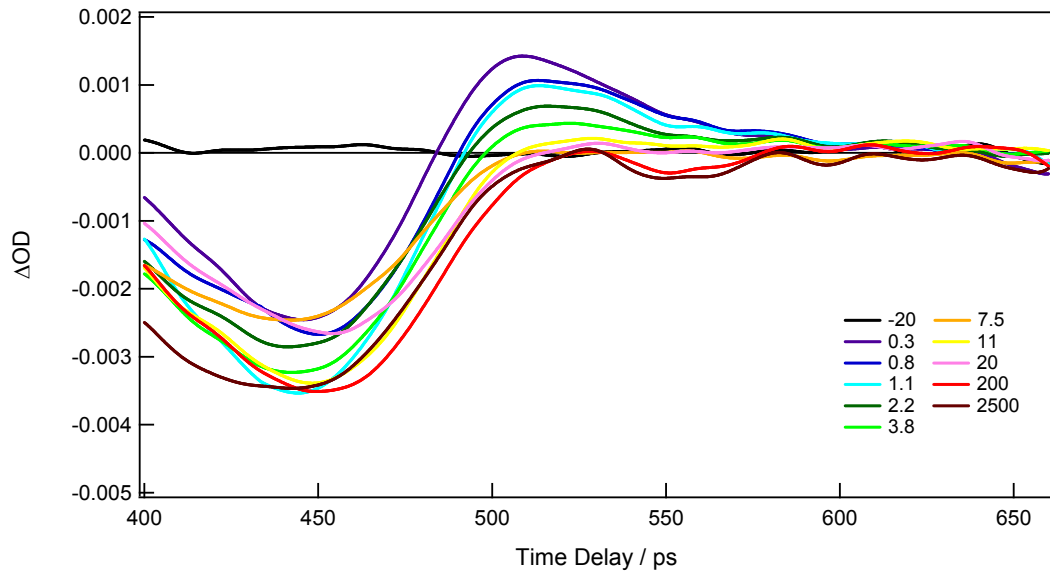


Figure S3. fsTA spectra of **1A** in THF with excitation at 350 nm.

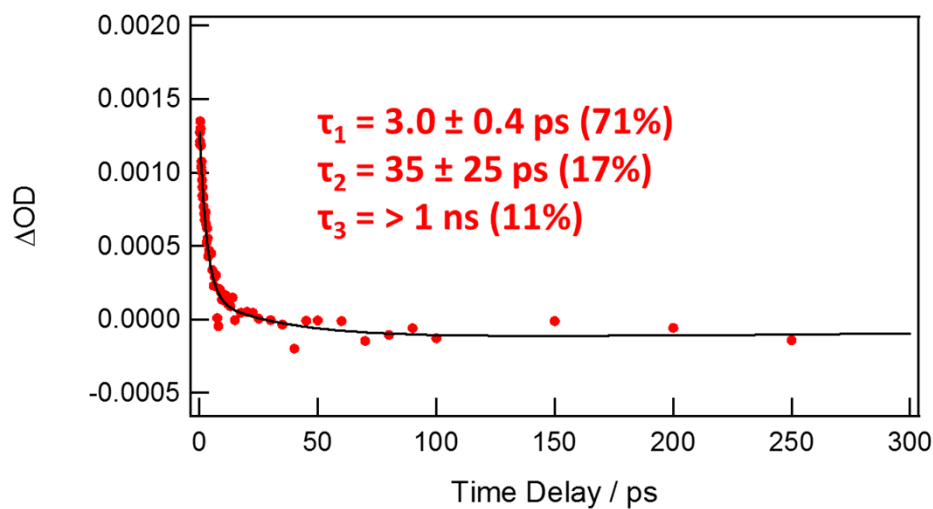


Figure S4. Kinetic trace from fsTA spectra of **1A** taken at 520 nm.

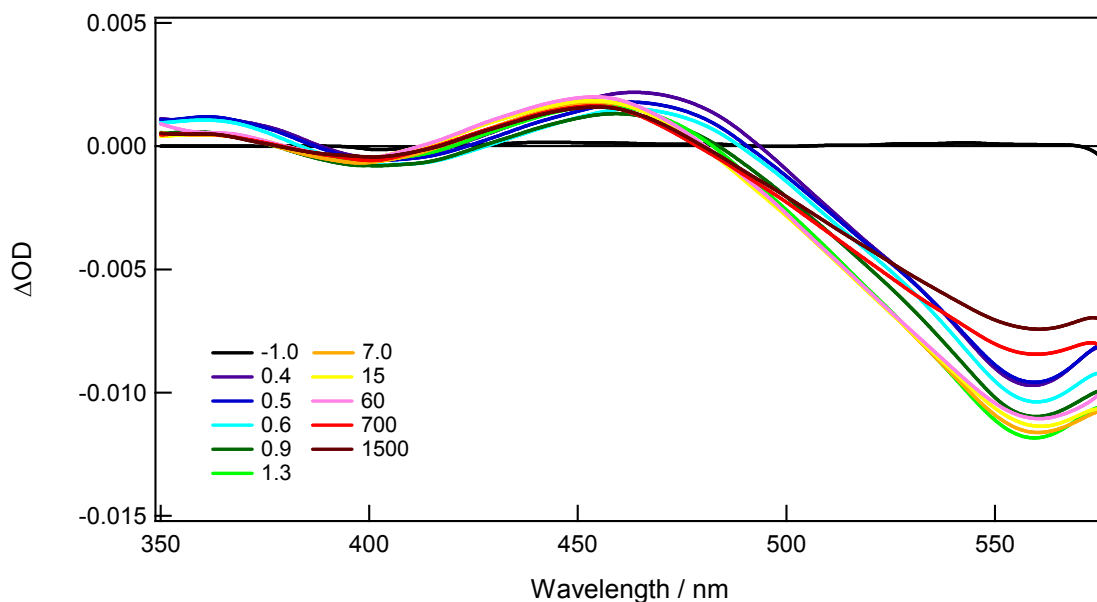


Figure S5. fsTA spectra of **1B** in THF with excitation at 600 nm.

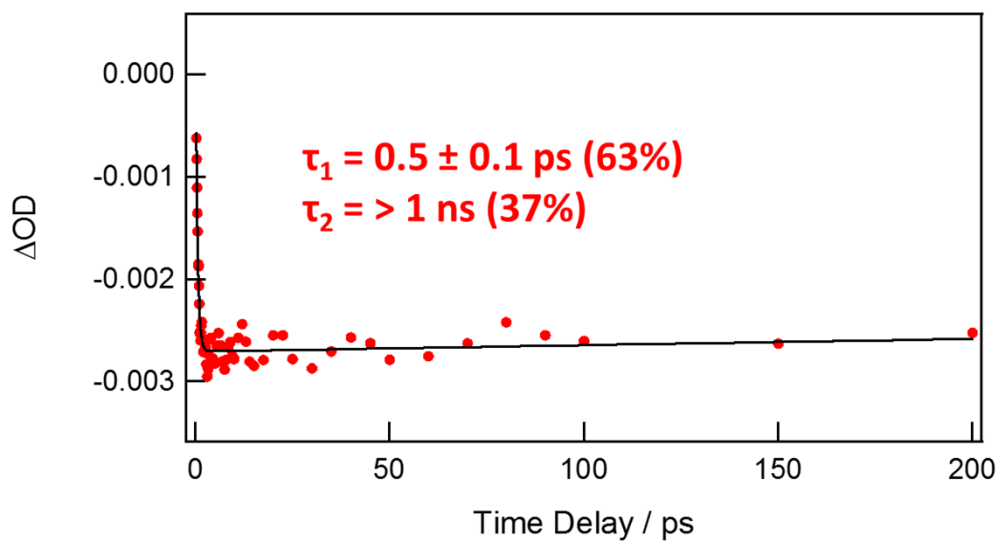
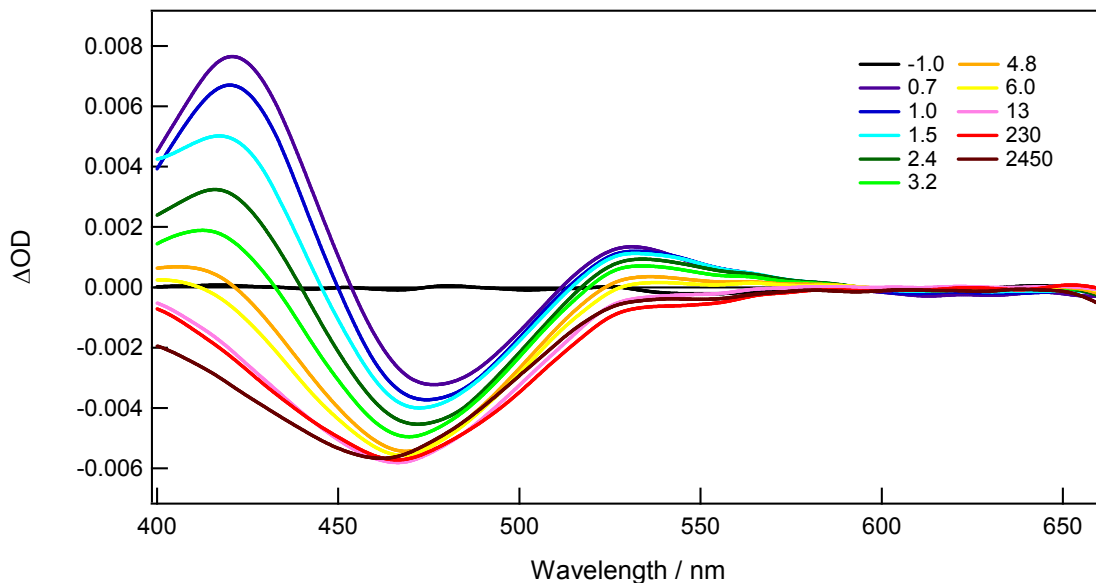


Figure S6. Kinetic trace from fsTA spectra of **1B** taken at 500 nm.



5

Figure S7. fsTA spectra of **2A** in THF with excitation at 350 nm.

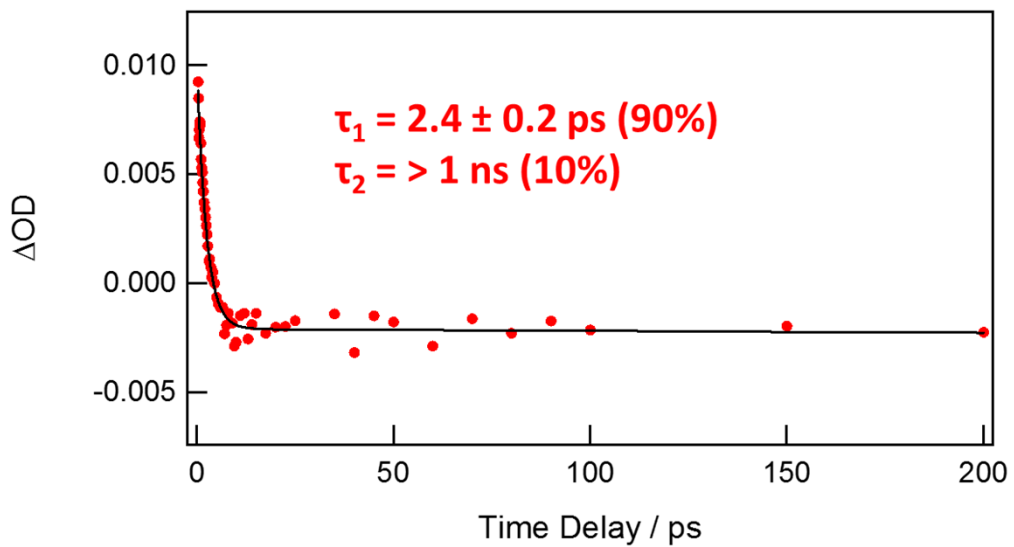


Figure S8. Kinetic trace from fsTA spectra of **2A** taken at 425 nm.

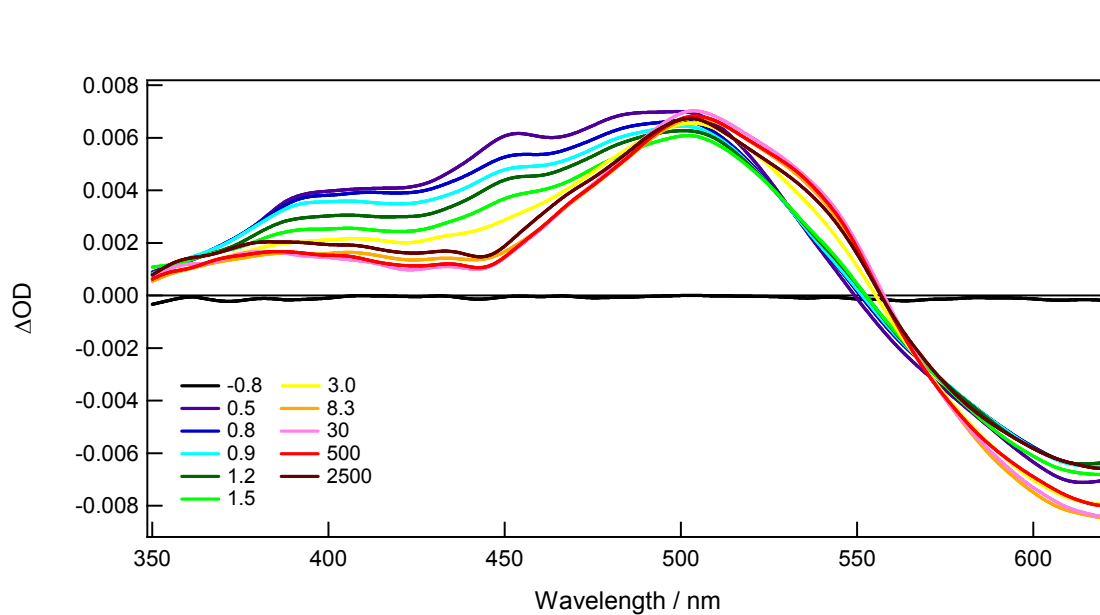


Figure S9. fsTA spectra of **2B** in THF with excitation at 675 nm.

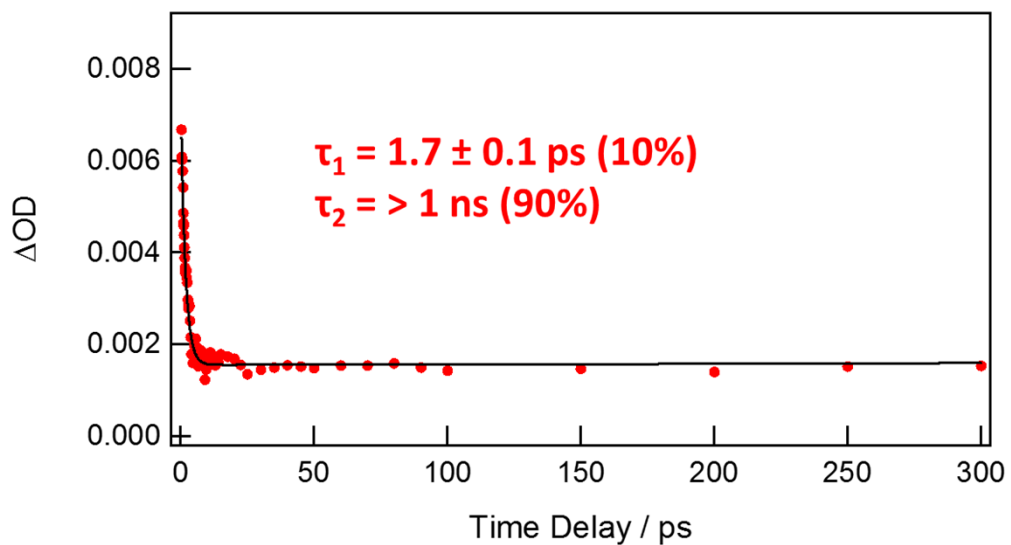


Figure S10. Kinetic trace from fsTA spectra of **2B** taken at 450 nm.

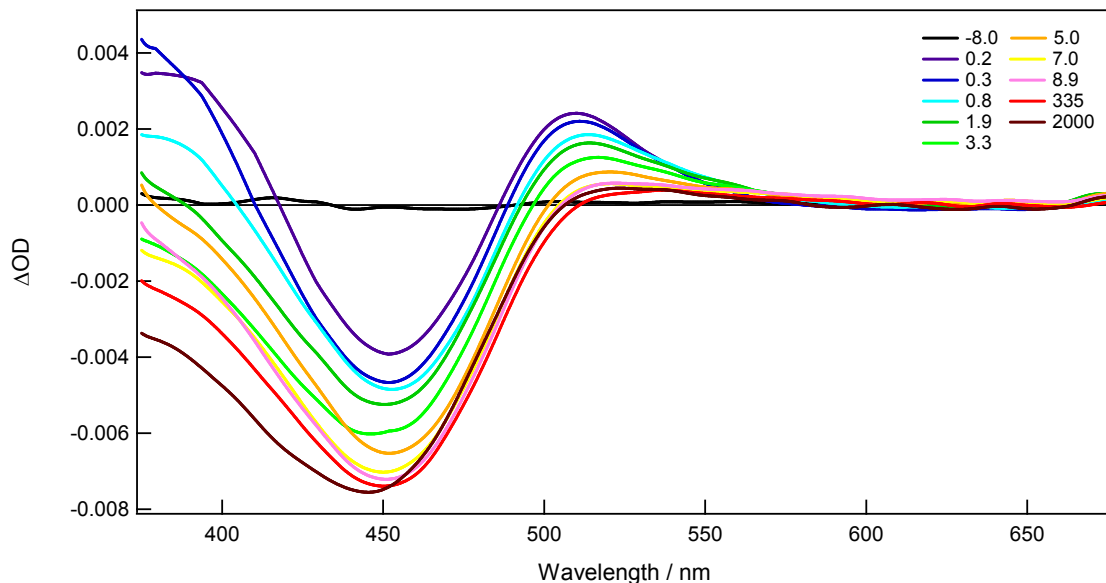


Figure S11. fsTA spectra of **3A** in THF with excitation at 350nm.

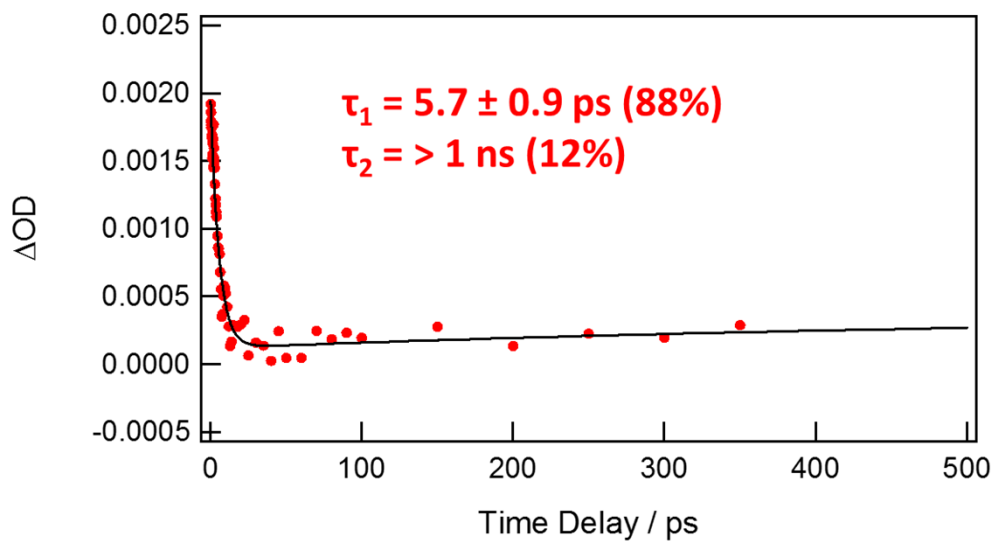


Figure S12. Kinetic trace from fsTA spectra of **3A** taken at 520 nm.

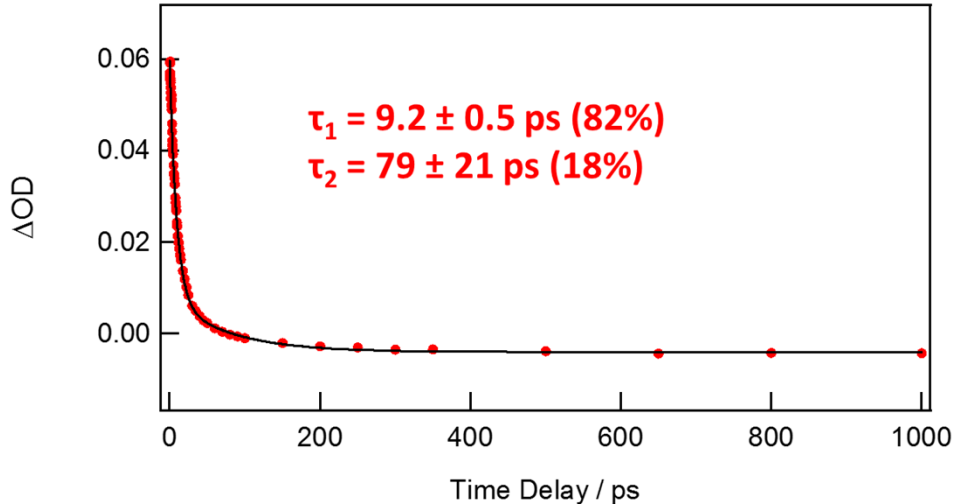


Figure S13. Kinetic trace from fsTA spectra of **4A** taken at 560 nm.

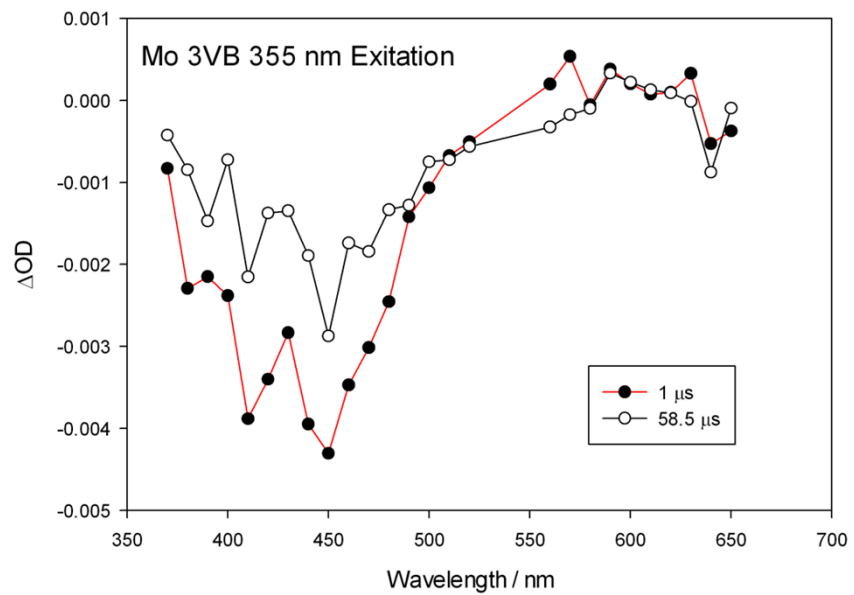


Figure S14. nsTA spectra of **1A** in THF with excitation at 355 nm.

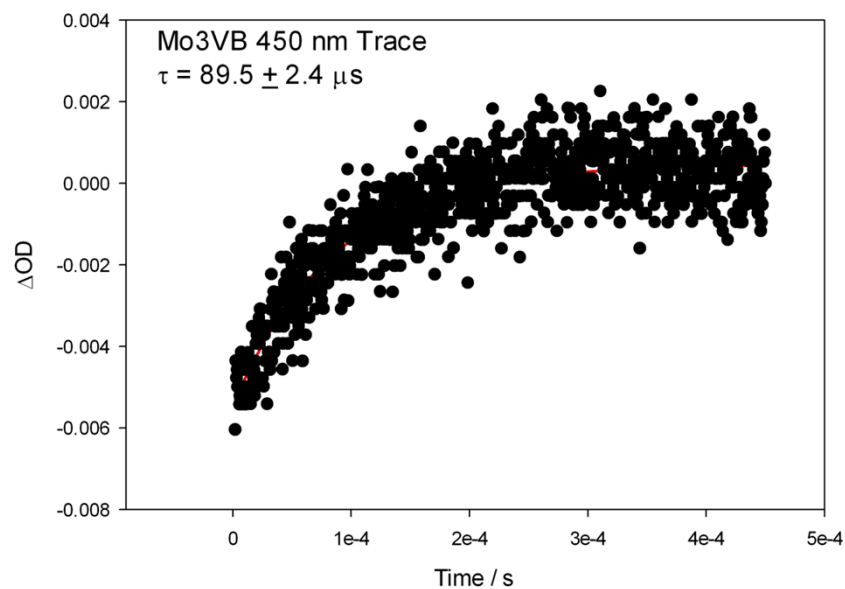


Figure S15. Kinetic trace from nsTA spectra of **1A** taken at 540 nm.

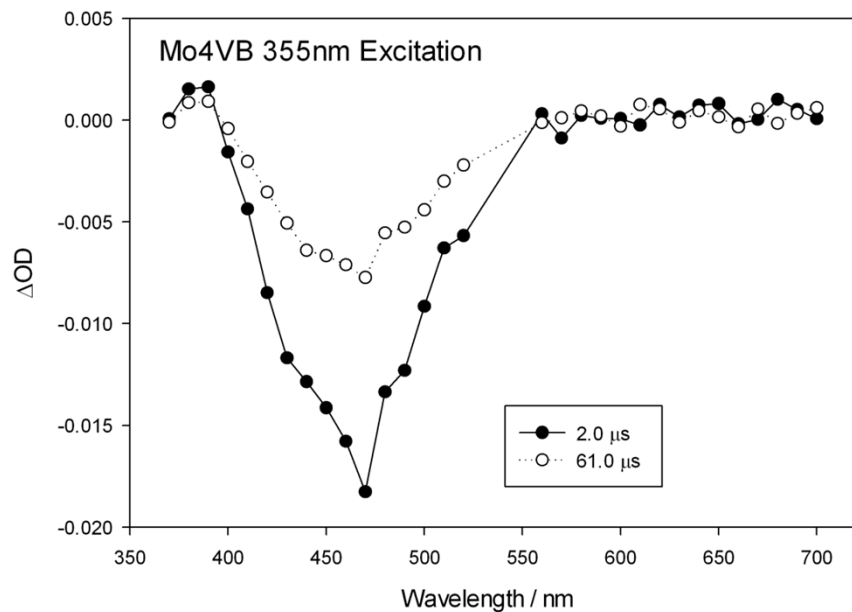


Figure S16. nsTA spectra of **2A** in THF with excitation at 355 nm.

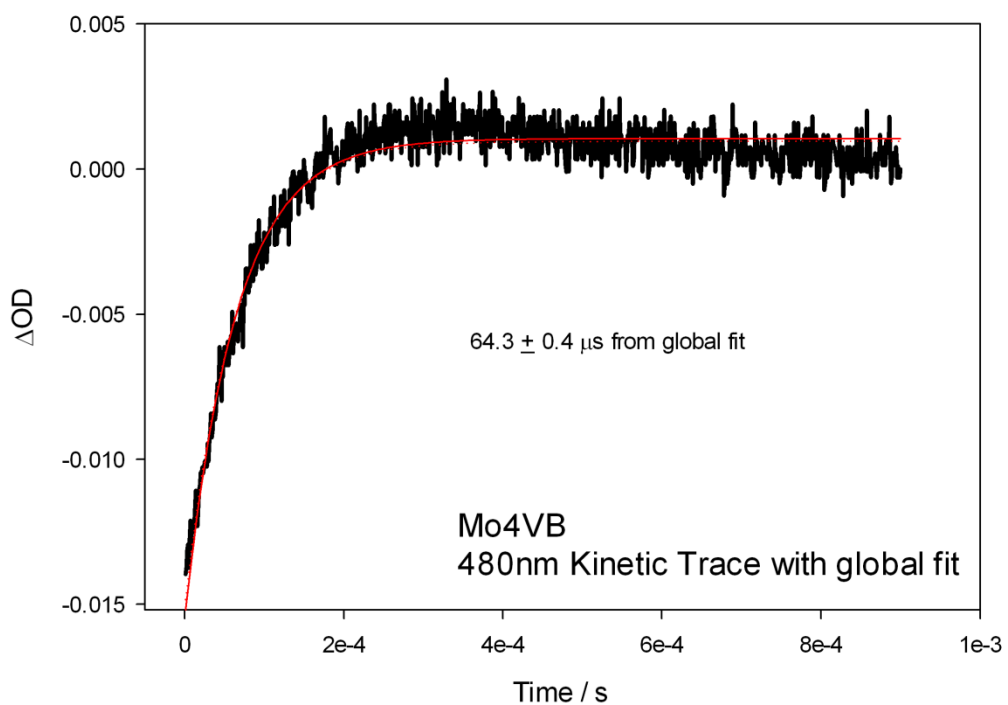


Figure S17. Kinetic trace from nsTA spectra of **2A** taken at 480 nm.

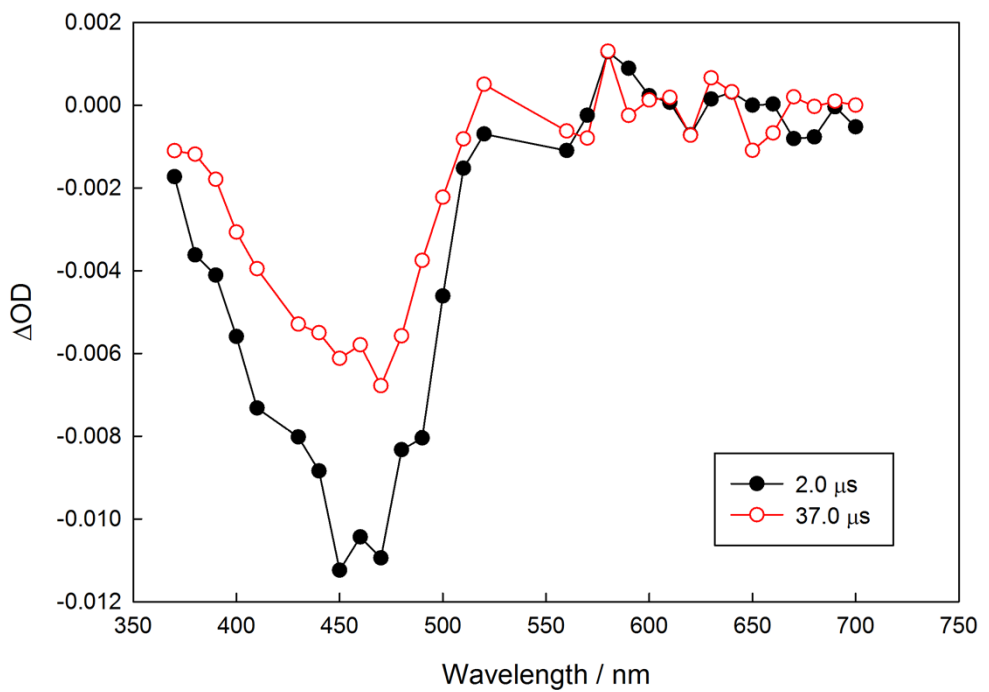


Figure S18. nsTA spectra of **3A** in THF with excitation at 355 nm.

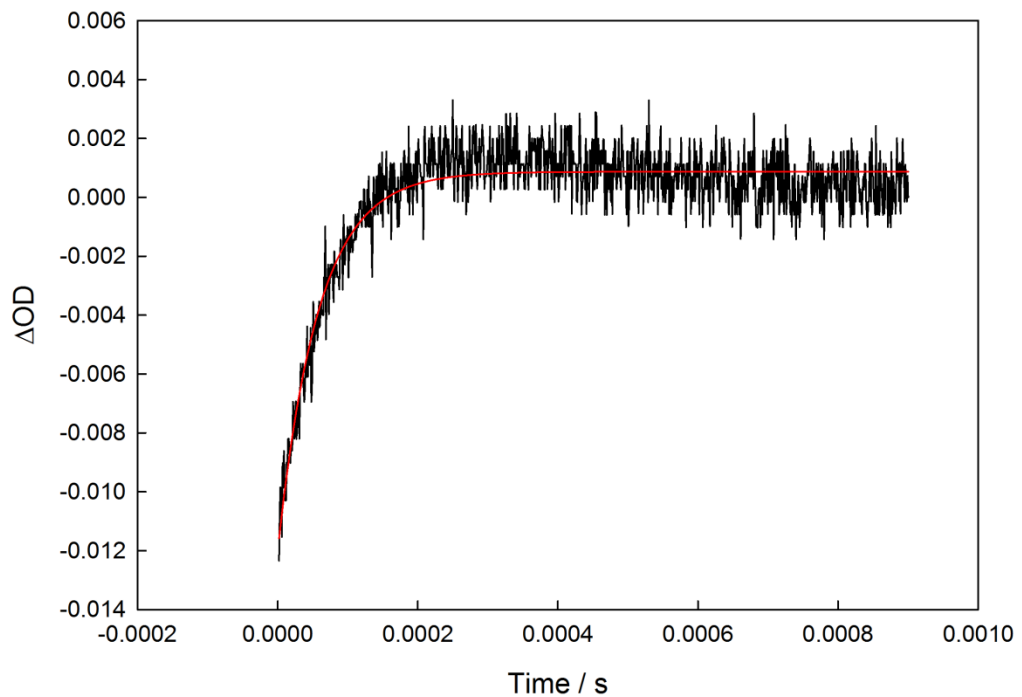


Figure S19. Kinetic trace from nsTA spectra of for **3A** taken at 480 nm.

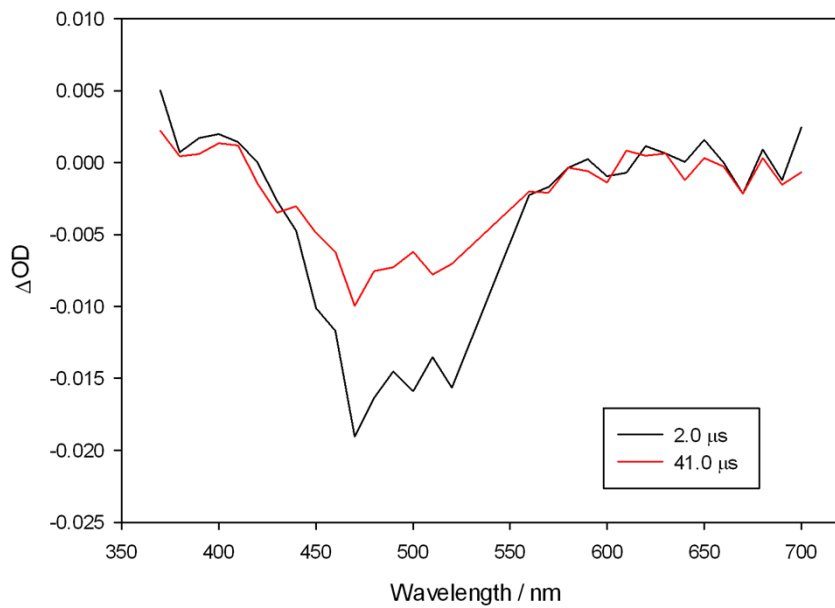


Figure S20. nsTA spectra of **4A** in THF with excitation at 355 nm.

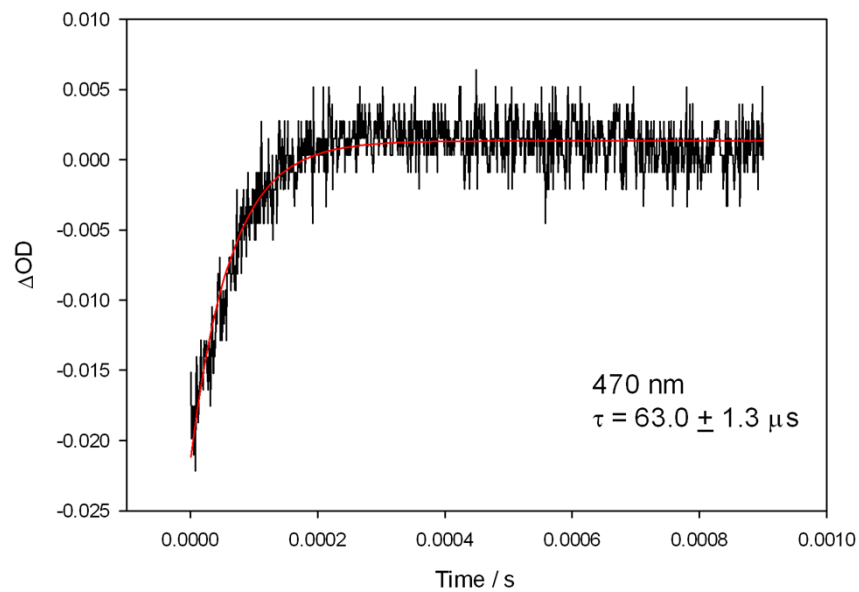


Figure S21. Kinetic trace from nsTA spectra of **4A** taken at 470 nm.

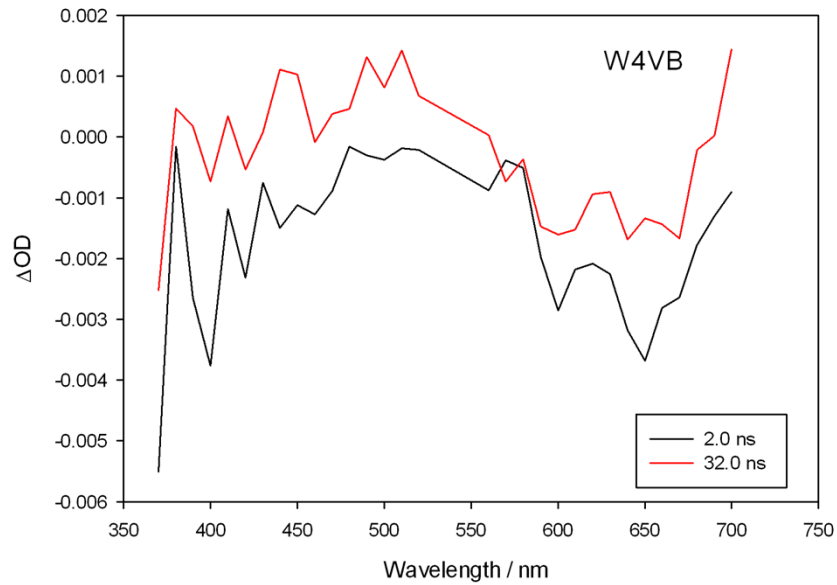


Figure S22. nsTA spectra of **2B** in THF with excitation at 355 nm.

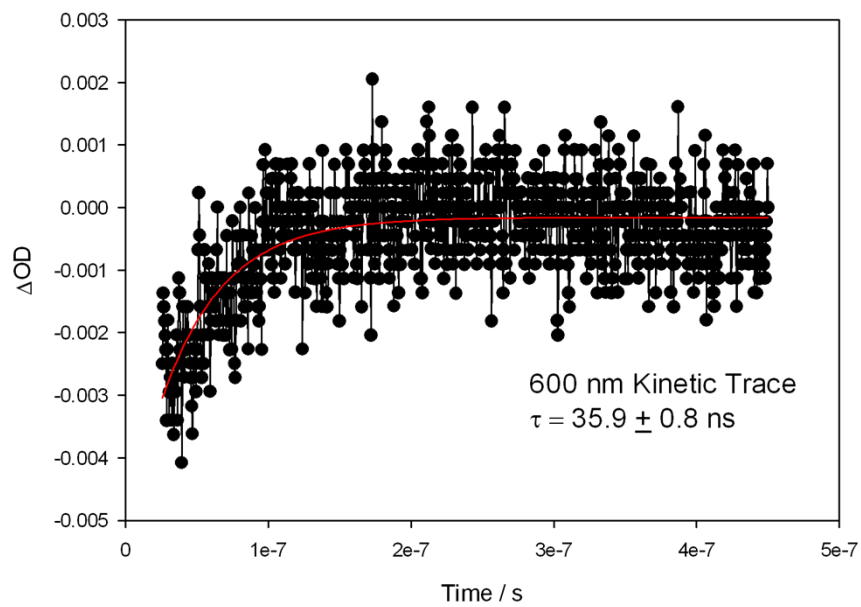


Figure S23. Kinetic trace from nsTA spectra of **2B** taken at 600 nm.

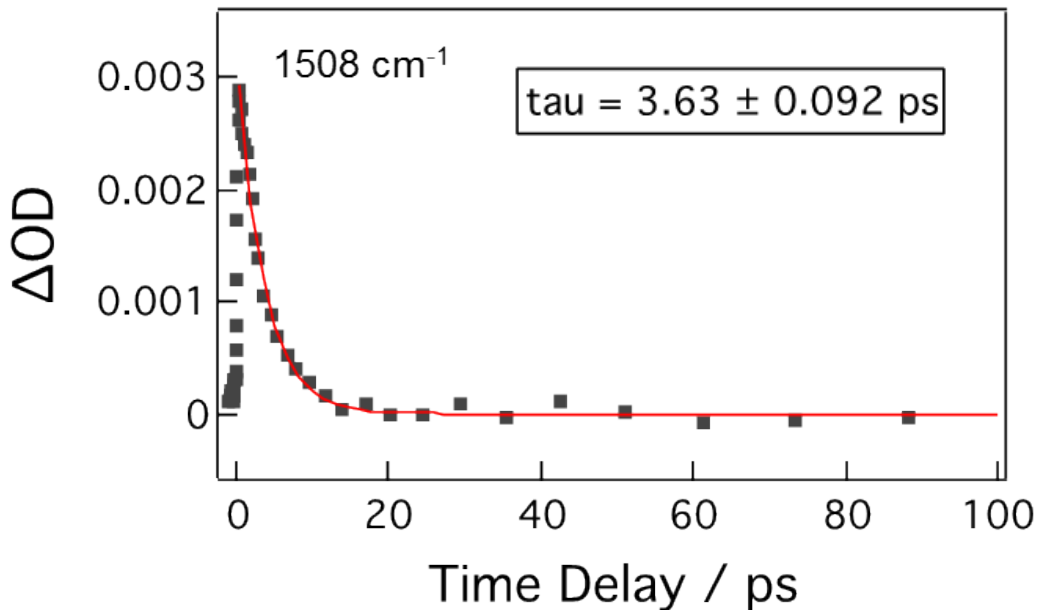


Figure S24. Kinetic trace from fsTRIR spectra of **2A** taken at  $1508\text{ cm}^{-1}$ .

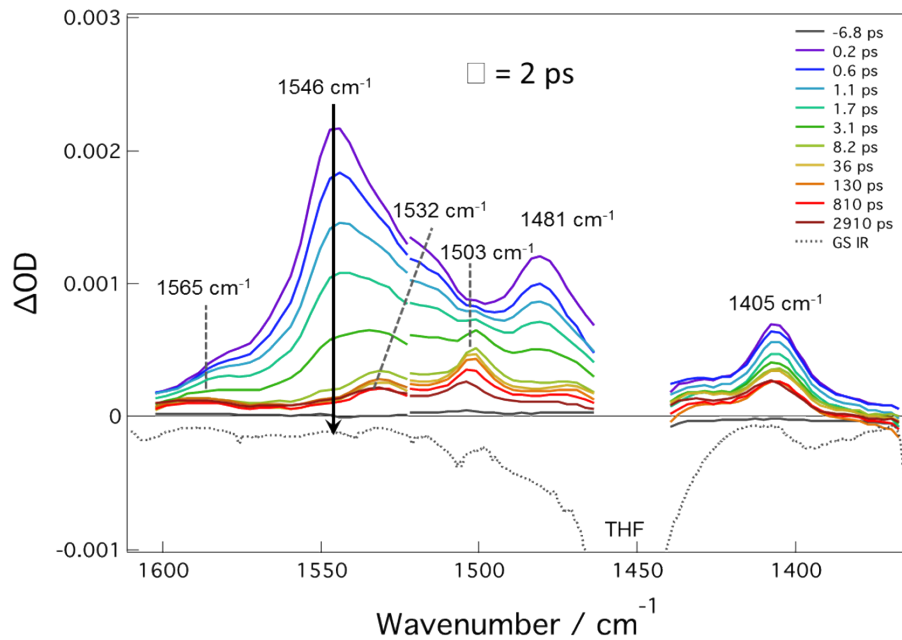


Figure S25. fsTRIR spectra of **2B** in THF with excitation at  $675\text{ nm}$ .

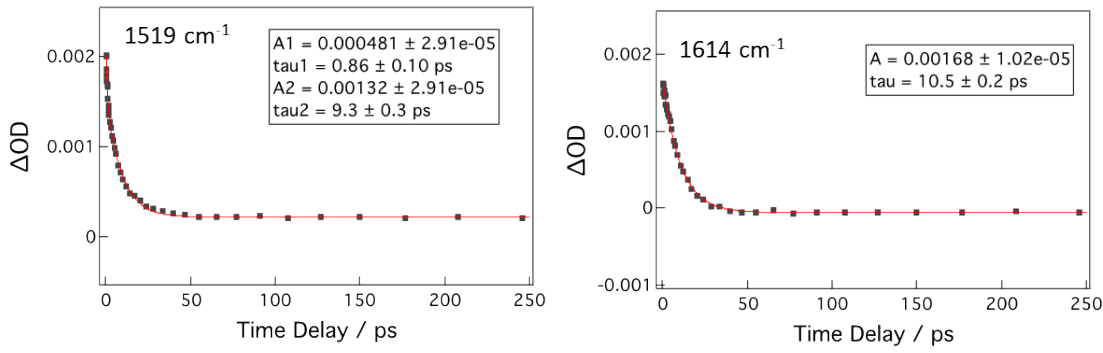


Figure S26. Kinetic traces from fsTRIR spectra of **4A** taken at  $1519\text{ cm}^{-1}$  and  $1614\text{ cm}^{-1}$ .

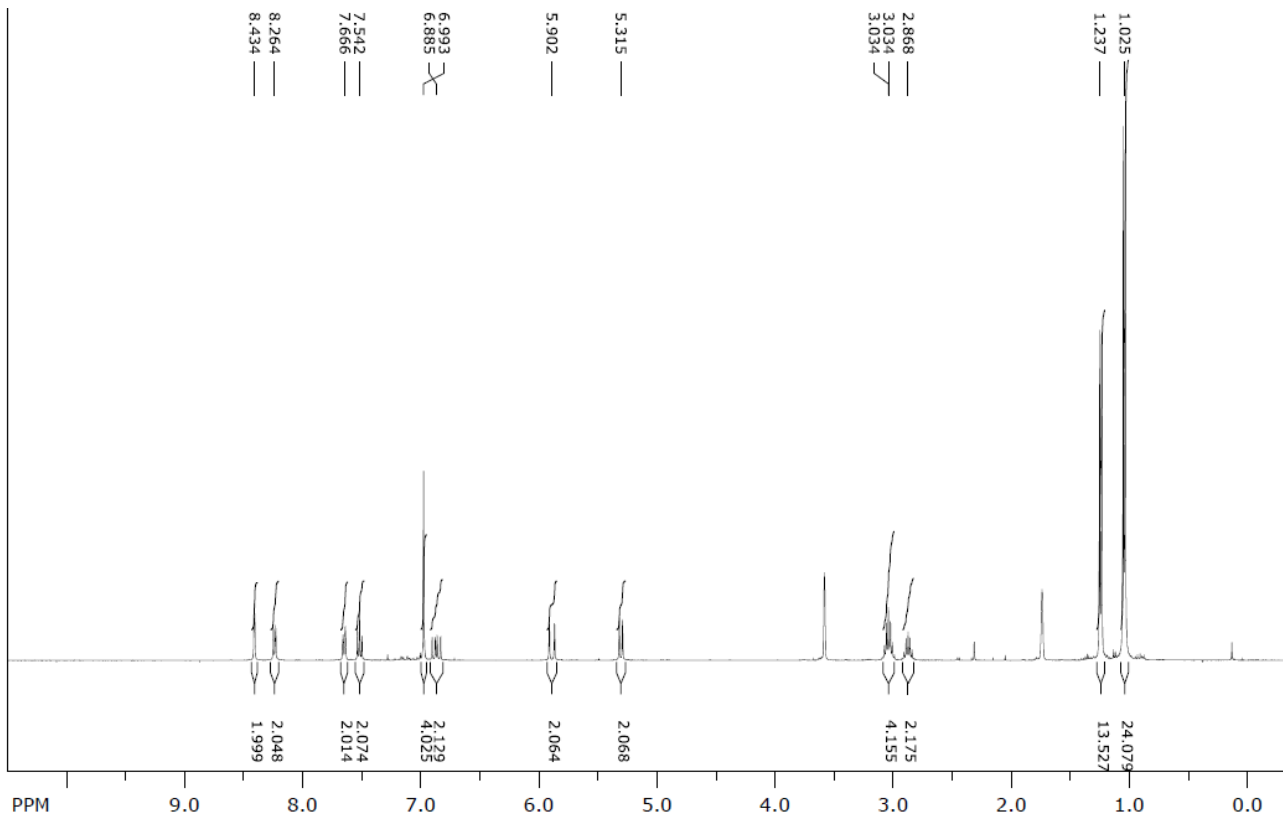


Figure S27. <sup>1</sup>H NMR of **1A** in <sup>d</sup><sub>8</sub>-THF (residual peaks: 3.58 and 1.73 ppm) at room temperature.

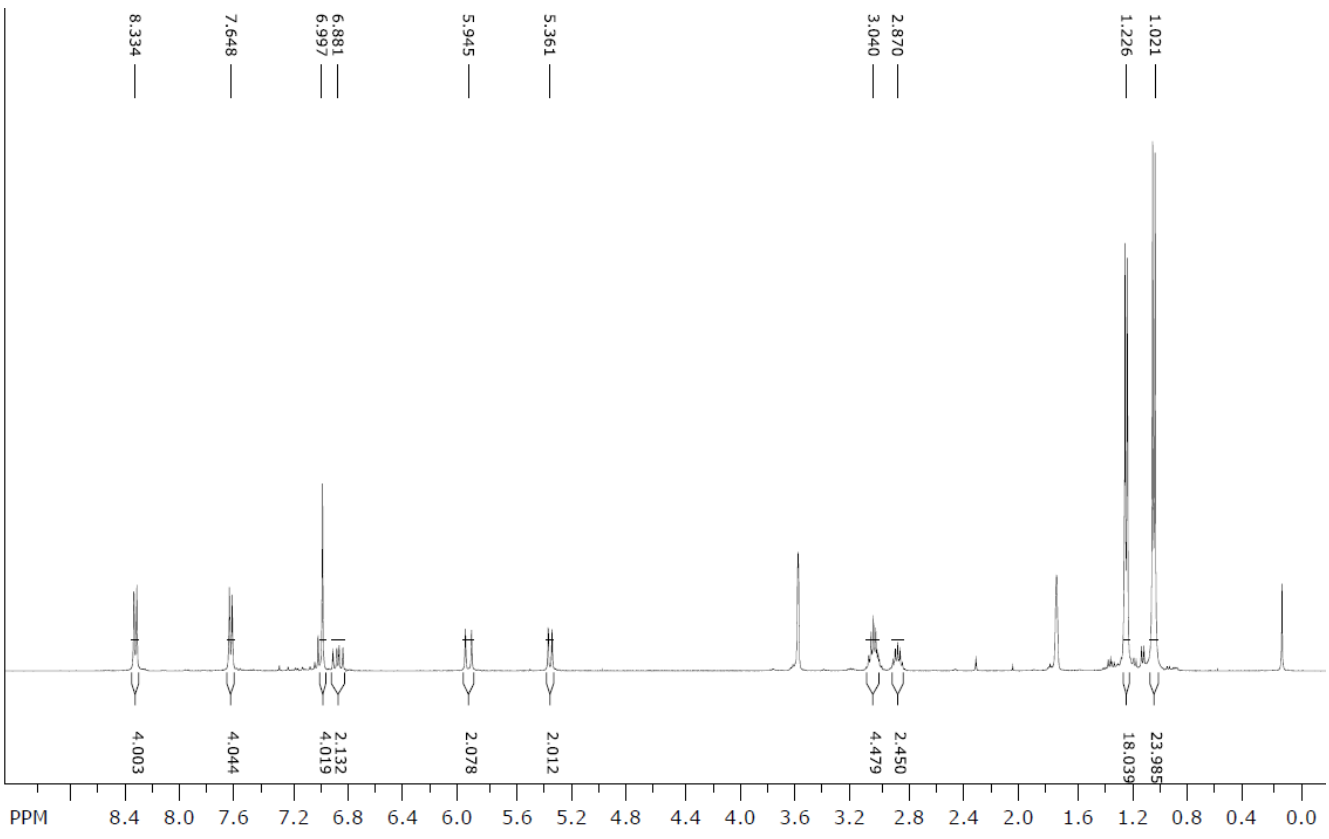


Figure S28.  ${}^1\text{H}$  NMR of **2A** in  $\text{d}_8\text{-THF}$  (residual peaks: 3.58 and 1.73 ppm) at room temperature.

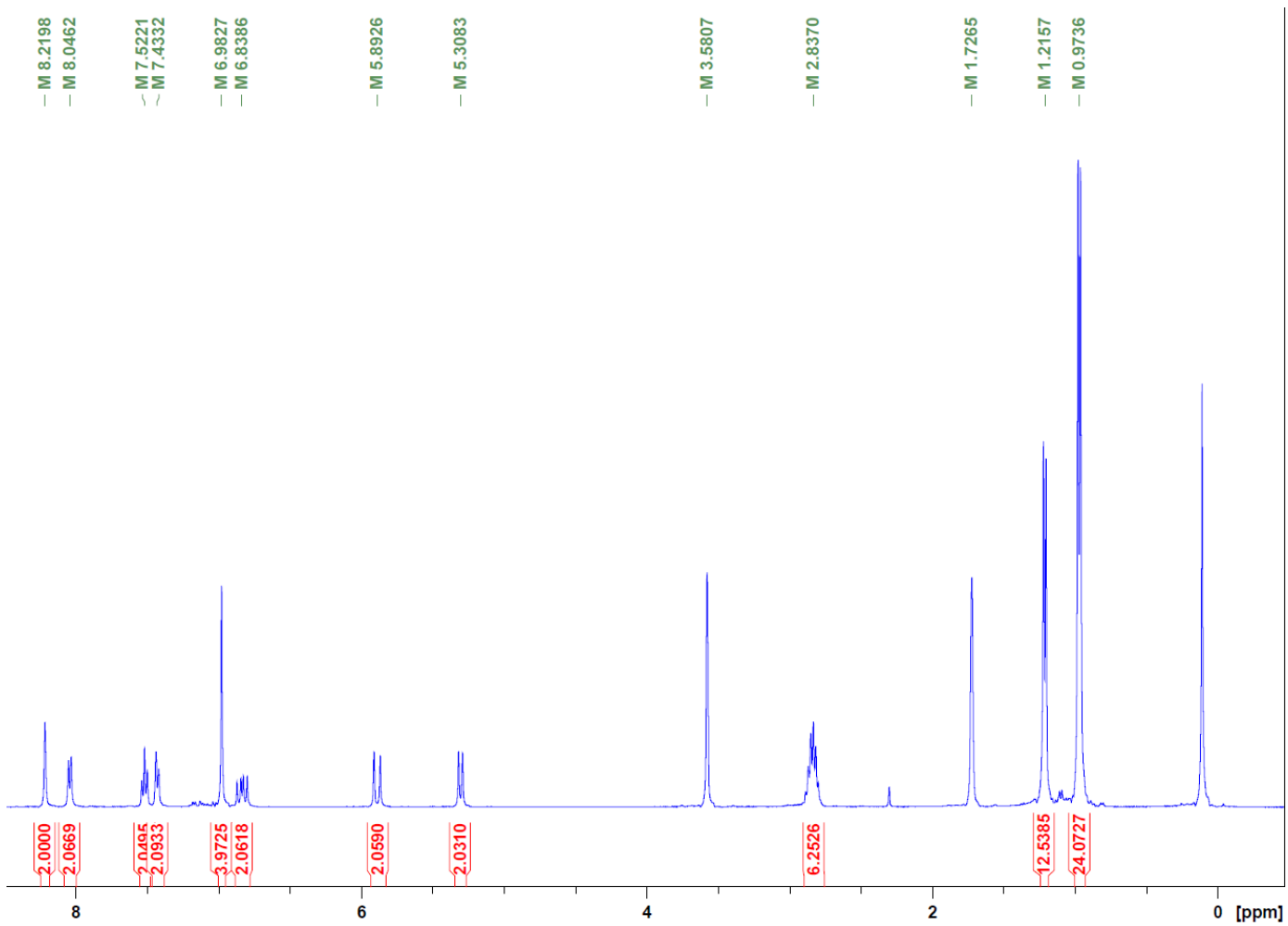


Figure S29  ${}^1\text{H}$  NMR of **1B** in  $\text{d}_8\text{-THF}$  (residual peaks: 3.58 and 1.73 ppm) at room temperature.

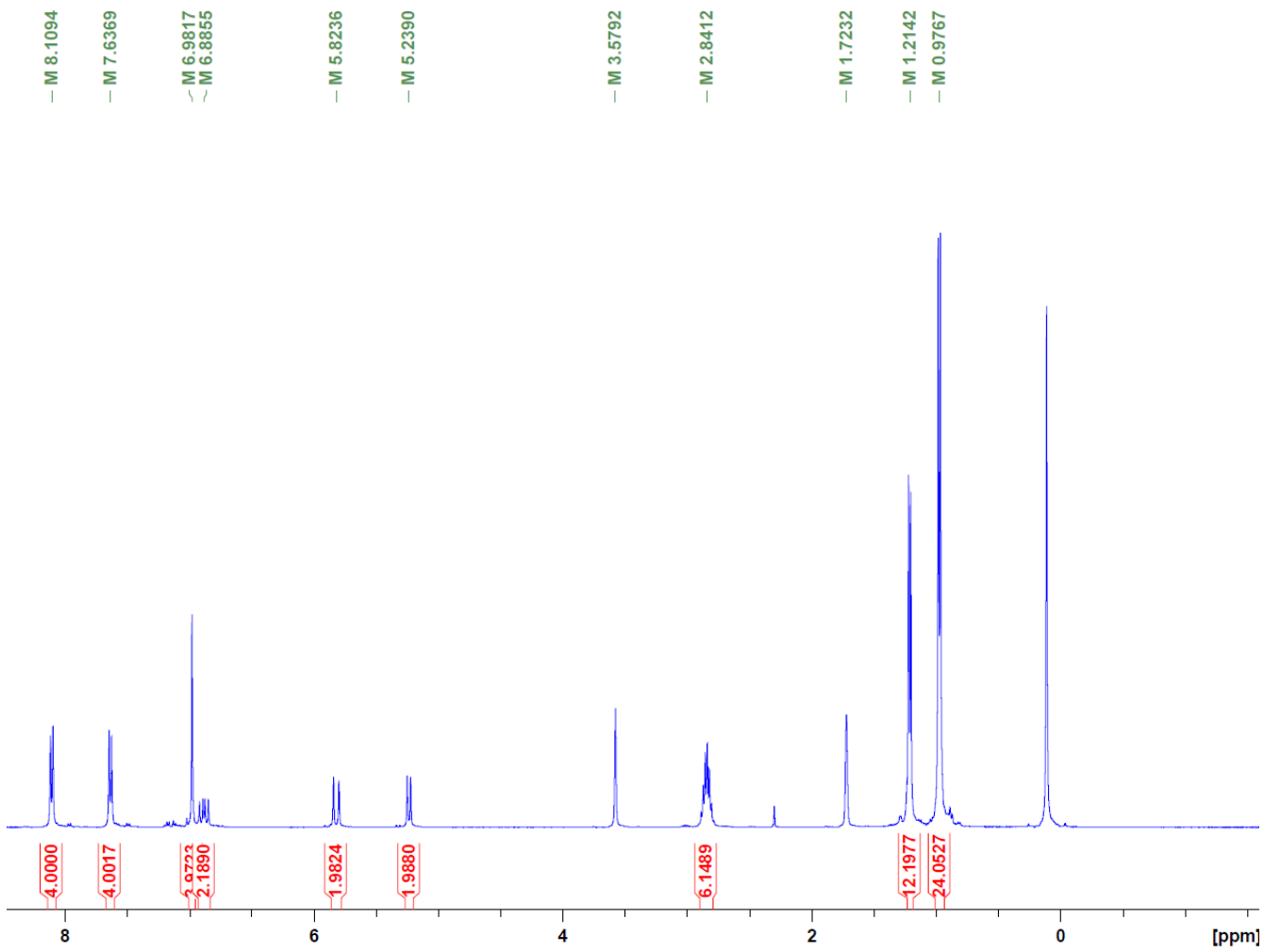


Figure S30. <sup>1</sup>H NMR of **2B** in  $d_8$ -THF (residual peaks: 3.58 and 1.73 ppm) at room temperature.

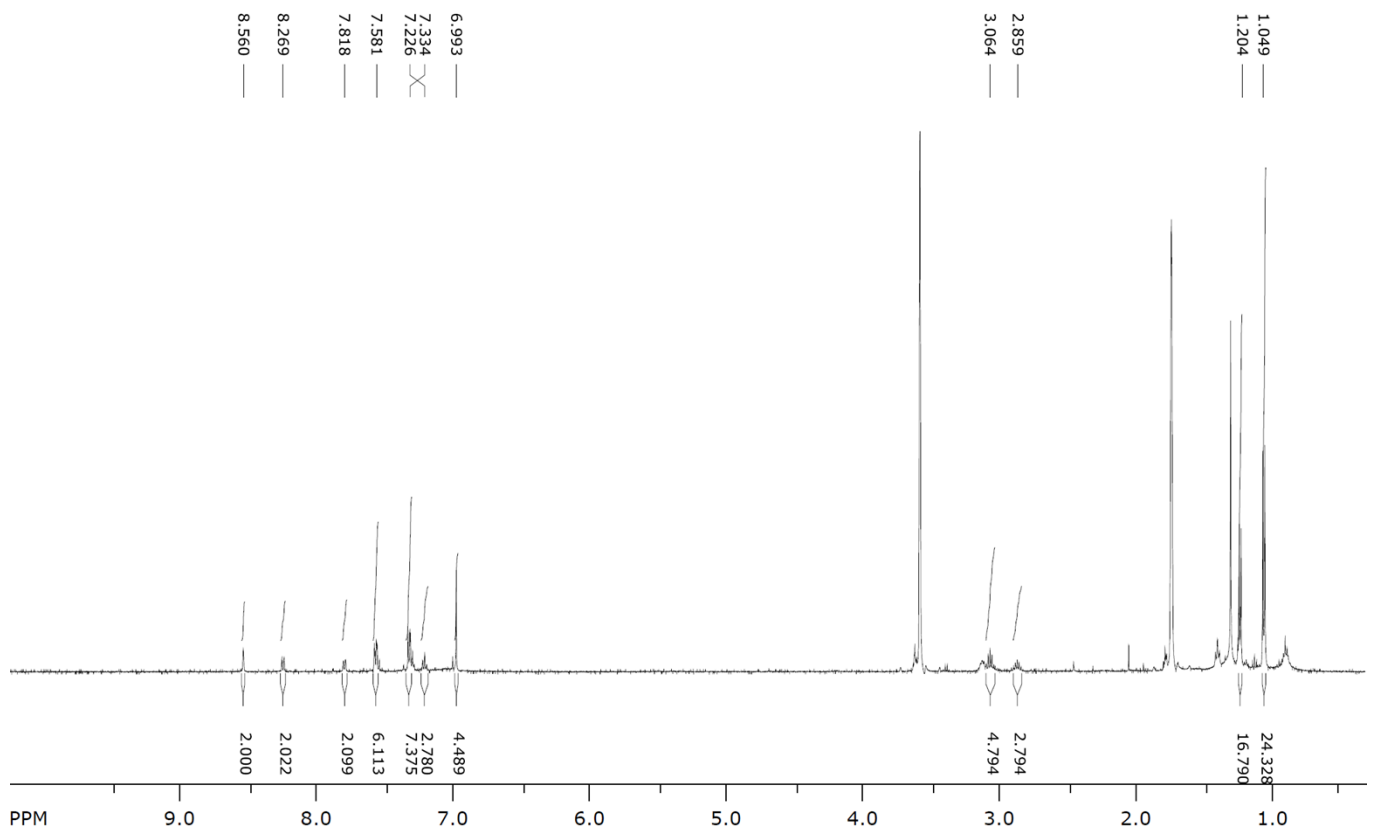


Figure S31. <sup>1</sup>H NMR of **3A** in *d*<sub>8</sub>-THF (residual peaks: 3.58 and 1.73 ppm) at room temperature. Small amounts of the catalyst, Pd(O<sub>2</sub>Ac)<sub>2</sub>, can also be seen in the spectra.

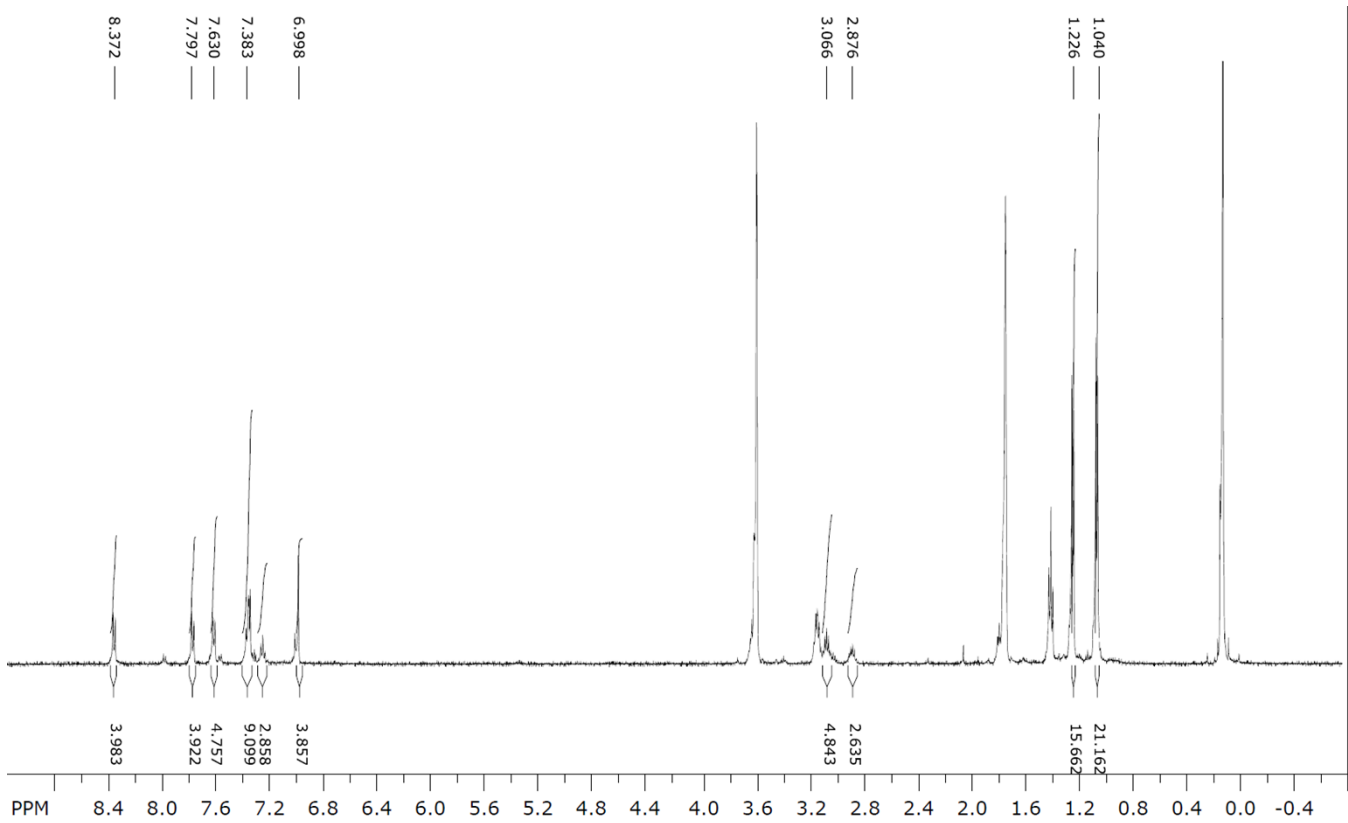


Figure S32.  ${}^1\text{H}$  NMR of **4A** in  $\text{d}_8\text{-THF}$  (residual peaks: 3.58 and 1.73 ppm) at room temperature. Small amounts of the base  $\text{N}(\text{Et})_3$  can also be seen in the spectrum.

Figure S33 High resolution MALDI-MS of **1A**.

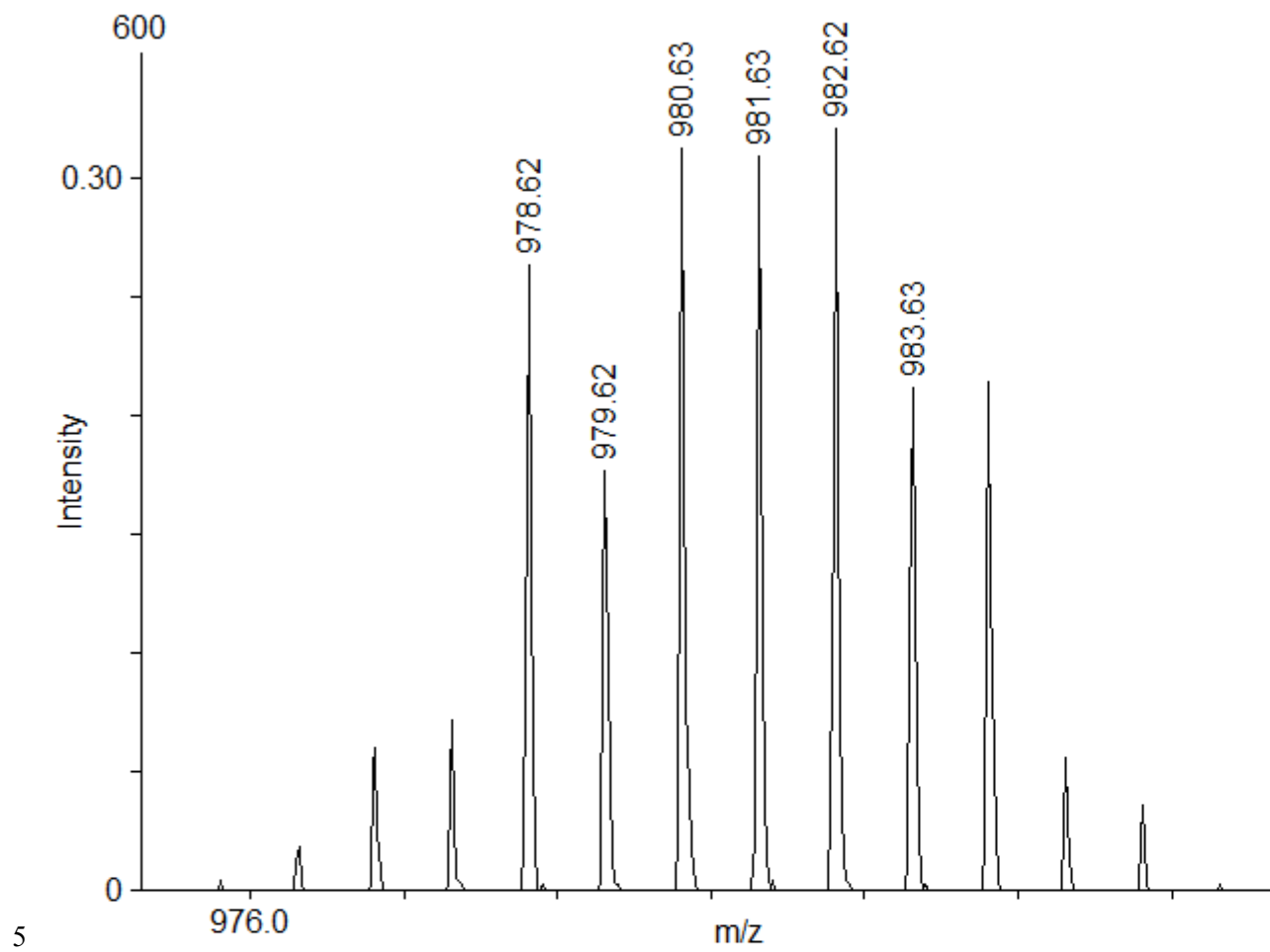


Figure S34 High resolution MALDI-MS of **1B**.

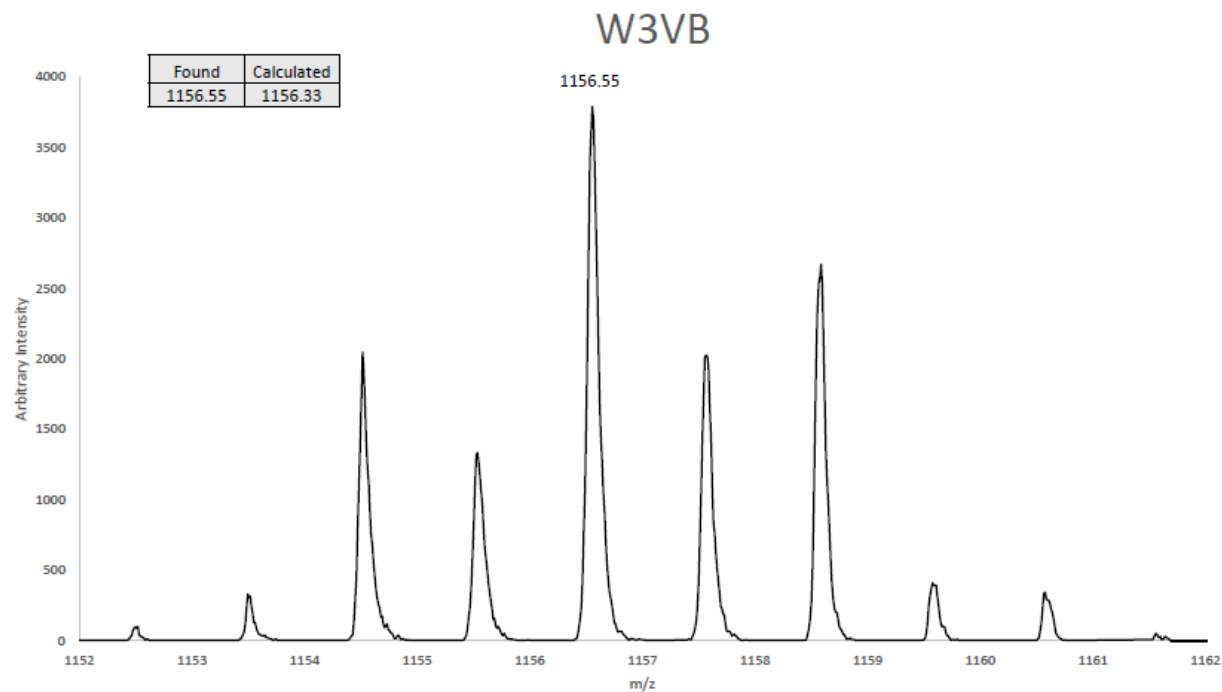


Figure S35 High resolution MALDI-MS of **2A**.

5

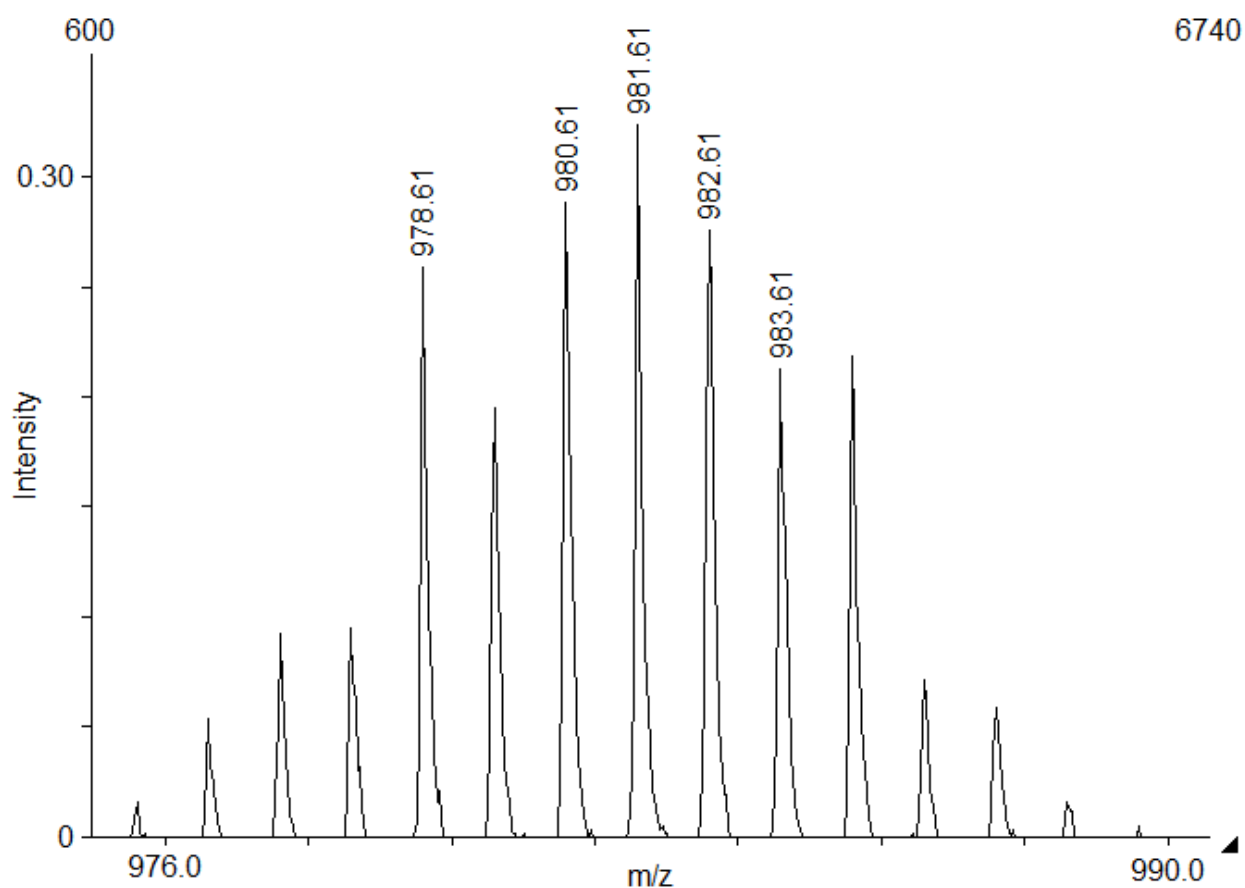


Figure S36 High resolution MALDI-MS of **2B**.

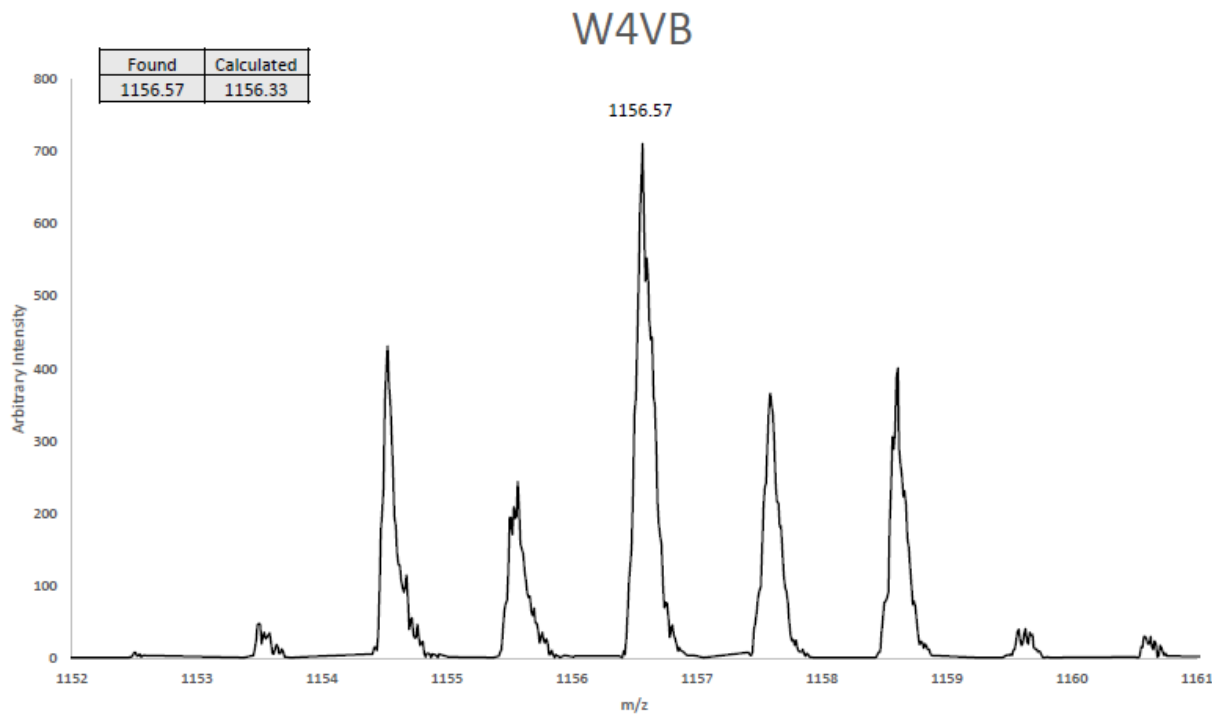


Figure S37 High resolution MALDI-MS of **3A**.

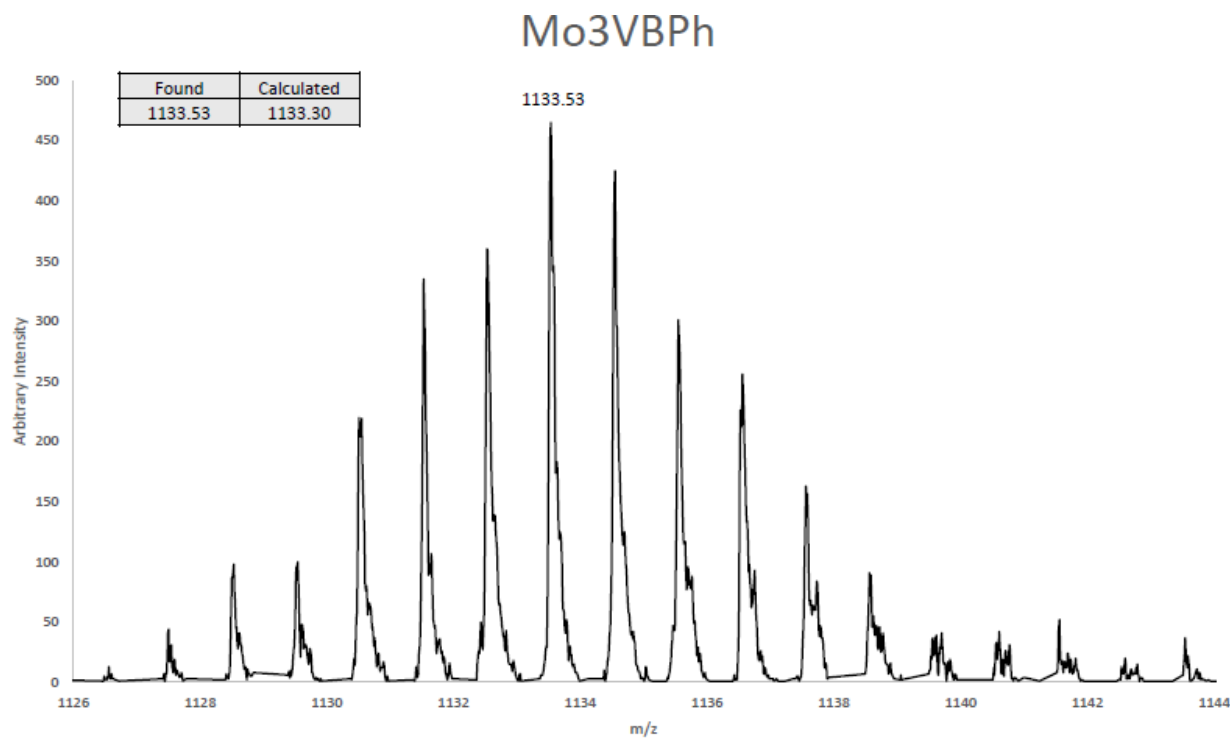


Figure S38 High resolution MALDI-MS of **4A**.

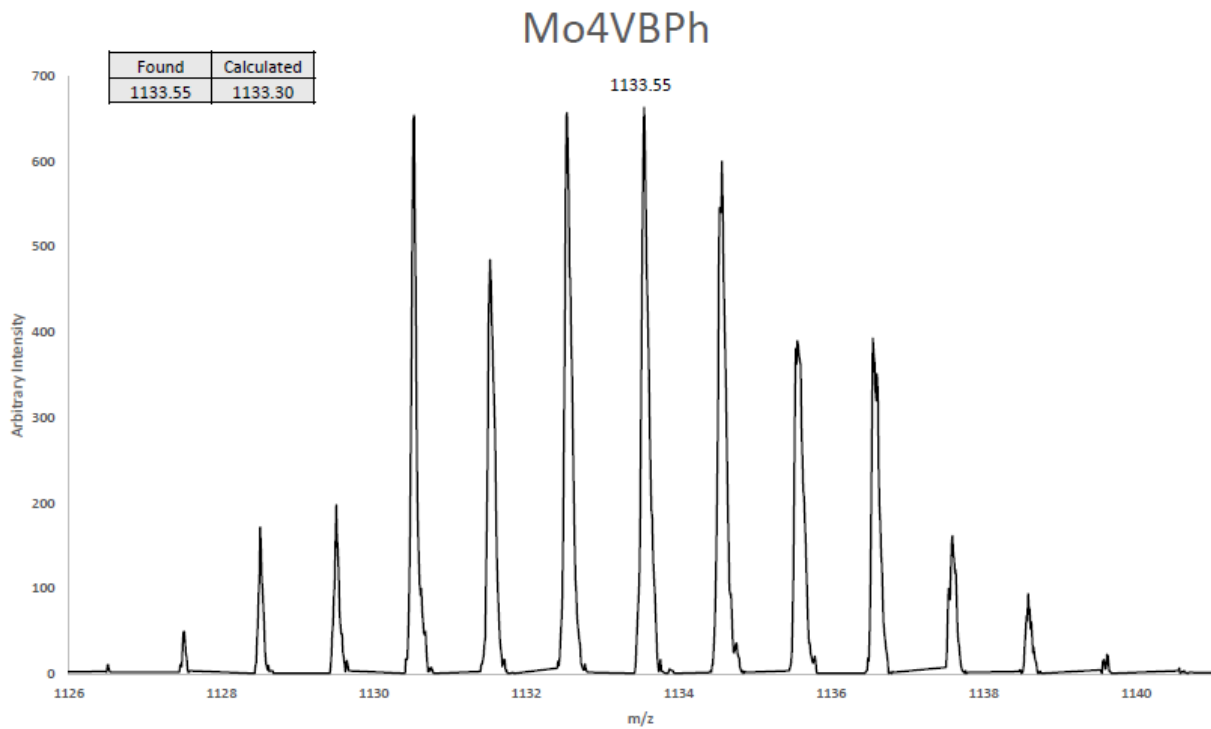


Table S39. Comparison of experimental and theoretical electronic transitions.

Compound	Transition	Experimental Absorption	Calculated Absorption (Oscillator Strength)	Orbital Contribution
<b>1A</b>	$^1\text{MLCT}$ ( $\text{Mo}_2 \rightarrow \text{T}^{\text{i}}\text{PB}$ )	337 nm	308 nm (0.1124)	$\text{HOMO} \rightarrow \text{LUMO}+8$
	$^1\text{MLCT}$ ( $\text{Mo}_2 \rightarrow 3\text{-VB}$ )	437 nm	424 nm (0.5379)	$\text{HOMO} \rightarrow \text{LUMO}+1$
<b>1B</b>	$^1\text{MLCT}$ ( $\text{W}_2 \rightarrow \text{T}^{\text{i}}\text{PB}$ )	401 nm	347 nm (0.1526)	$\text{HOMO} \rightarrow \text{LUMO}+6$
	$^1\text{MLCT}$ ( $\text{W}_2 \rightarrow 3\text{-VB}$ )	563, 601 nm	495 nm (0.6684)	$\text{HOMO} \rightarrow \text{LUMO}$
<b>2A</b>	$^1\text{MLCT}$ ( $\text{Mo}_2 \rightarrow \text{T}^{\text{i}}\text{PB}$ )	335 nm	309 nm (0.1099)	$\text{HOMO} \rightarrow \text{LUMO}+6$
	$^1\text{MLCT}$ ( $\text{Mo}_2 \rightarrow 4\text{-VB}$ )	467 nm	459 nm (0.7307)	$\text{HOMO} \rightarrow \text{LUMO}$
<b>2B</b>	$^1\text{MLCT}$ ( $\text{W}_2 \rightarrow \text{T}^{\text{i}}\text{PB}$ )	405 nm	349 nm (0.1488)	$\text{HOMO} \rightarrow \text{LUMO}+4$
	$^1\text{MLCT}$ ( $\text{W}_2 \rightarrow 4\text{-VB}$ )	605, 652 nm	537 nm (0.8937)	$\text{HOMO} \rightarrow \text{LUMO}$
<b>3A</b>	$^1\text{MLCT}$ ( $\text{Mo}_2 \rightarrow \text{T}^{\text{i}}\text{PB}$ )	318 nm	298 nm (0.1136)	$\text{HOMO} \rightarrow \text{LUMO}+8$
	$^1\text{MLCT}$ ( $\text{Mo}_2 \rightarrow 3\text{-VBPh}$ )	427 nm	373 nm (0.2926) 434 nm (0.5829)	$\text{HOMO} \rightarrow \text{LUMO}$ $\text{HOMO} \rightarrow \text{LUMO}+1$ $\text{HOMO} \rightarrow \text{LUMO}+3$
<b>4A</b>	$^1\text{MLCT}$ ( $\text{Mo}_2 \rightarrow \text{T}^{\text{i}}\text{PB}$ )	318 nm	345 nm (1.3354)	$\text{HOMO} \rightarrow \text{LUMO}+6$ $\text{HOMO-1} \rightarrow \text{LUMO}+1$ $\text{HOMO-2} \rightarrow \text{LUMO}$
	$^1\text{MLCT}$ ( $\text{Mo}_2 \rightarrow 4\text{-VBPh}$ )	486 nm	498 nm (1.2129)	$\text{HOMO} \rightarrow \text{LUMO}$

Table S40. Crystallographic Data Collection Parameters for **1A** and **2A**

Compound	<b>1A</b>	<b>2A</b>
Chemical Formula	C <sub>58</sub> H <sub>76</sub> Mo <sub>2</sub> O <sub>10</sub>	C <sub>58</sub> H <sub>76</sub> Mo <sub>2</sub> O <sub>10</sub>
Formula Weight	1125.06	1125.06
Temperature (K)	150(2)	150(2)
Space Group	Monoclinic, P2 <sub>1</sub> /c	Triclinic, P-1
<i>a</i> (Å)	9.9404(3)	9.8343(2)
<i>b</i> (Å)	15.7440(4)	11.2520(2)
<i>c</i> (Å)	17.7587(4)	15.7140(3)
$\alpha$ (°)		107.000(1)
$\beta$ (°)	100.059(1)	105.165(1)
$\gamma$ (°)		90.114(1)
V (Å <sup>3</sup> )	2736.54 (12)	1599.14(5)
Z	2	1
D <sub>calcd</sub> (Mg/m <sup>3</sup> )	1.365	1.168
Crystal Size (mm)	0.38 X 0.19 X 0.19	0.23 X 0.23 X 0.15
Theta range for data collection	1.740 to 27.433°	1.899 to 27.467°
$\mu$ (mm <sup>-1</sup> ) [Mo, K $\alpha$ ]	0.514	0.440
F(000)	1176	588
Reflections collected	49649	46246
Unique reflections	6233 [R(int)= 0.051]	7310 [R(int)= 0.038]
Data Completeness to [ θ ]	100% [25.242]	100% [25.242]
Data/restraints/parameters	6233 / 25 / 343	7310 / 1 / 326
R1 <sup>a</sup> (%) (all data)	5.06 (7.19)	3.79 (4.96)
wR2 <sup>b</sup> (%) (all data)	11.86 (13.19)	9.78 (10.38)
Goodness-of-fit on F <sup>2</sup>	1.058	1.060
Largest diff. peak and hole (e Å <sup>-3</sup> )	1.538 and -0.715	0.559 and -0.477

$$^a\text{R1} = \Sigma |F_o| - |F_c| / \Sigma |F_o| \times 100$$

$$^b\text{wR2} = [\sum w (F_o^2 - F_c^2)^2 / \sum (w |F_o|^2)^2]^{1/2} \times 100$$